Effect of The DC Traction Substations No-Load Voltage Set Up Over The System Efficiency

Bassam Mohamed
LEMUR Group
University of Oviedo
mohamedbassam@uniovi.es

Islam El-Sayed
LEMUR Group
University of Oviedo
islam@uniovi.es

Pablo Arboleya
LEMUR Group
University of Oviedo
arboleyapablo@uniovi.es

Clément Mayet
SATIE Laboratory
Le CNAM Paris
clement.mayet@lecnam.net

***Abstract*---The DC traction networks are widely used for urban transportation and short distances. The DC substations transfer the power between the main AC grid and the DC network. The open circuit voltage of the DC substation may be fixed based on the tap changer configuration of the transformer or using a dynamic control over the AC/DC converter. This article studies the effects of the selection of this voltage over the network performance which can be represented by the overall energy efficiency of the system. The simulation models are simplified to speed up the solver under the consideration of the required accuracy. The Aggregated data are used to reduce the storage requirements to save the results of all simulations. This study represents a systematic procedure for selecting the substation voltage to reduce the total losses of the system. The results of the testing on a real case demonstrates the improvement in the overall energy efficiency and the reduction of the total losses.**

***Index Terms* -- Electrical Railway Systems, Power Flow, DC Traction Networks, Railway.**

I. Introduction

In worldwide, mass transportation is shifted from fossil fuel to clean renewable electrical energy to overcome the pollution and the limitation of natural resources. The DC traction networks represent an effective sustainable solution for urban and short distances transportation. The new technology of energy storage and regenerative braking improve the overall energy efficiency of the DC traction network [1], [2].

Solving the power flow of the traction network is challenging because of the dynamic variation of the network topology and the power injection [3], [4]. The network model needs to be updated dynamically at each instant of the simulation based on the positions of the trains. Additional problems appear in the DC traction network because of the non-smooth characteristics of power electronic devices used in rectifiers and voltage control. Conventional solvers are not designed for solving this problem because they depend on the derivatives which are undefined at the breakpoints [5]. Smoothing functions can be used to avoid discontinuity in the derivative function. However, this method can slow down the simulation because of the higher calculation cost of the smoothing functions. Even though smooth equations may cause divergence and oscillation in some cases due to the variation of the derivative around the critical points [6]. This nonlinear and non-smooth problem can be solved using special iterative methods [6], [7]. Each iteration can be modeled with a linear approximation such as MNA (Modified Nodal Analysis) which is based on Kirchhoff laws of voltage and current [8], [9]. This linear system can be solved by direct factorization such as Zollenkopf, LU and Cholesky [10], [11]. The solvers update the unknown vector until the mismatch error is less than a given tolerance.

Some simulation methods use a unified AC and DC power flow model to represent the interaction between the AC grid and the DC network [12]--[15]. Even more detailed dynamic models of devices can be used to represent transient behavior of the real models of substation and trains [16]. Although, this kind of model improves the accuracy of the results it extends the simulation time. Other methods improve the simulation speed with acceptable accuracy by using simplified steady state models [3], [9], [11]. The train models can be represented as constant current or constant power sources. The constant current has a fast convergence rate because they are completely linear but the power sources are much accurate. The reference of the mechanical power can be calculated independently using the mechanical simulators based on the parameters of the trains, tracks, and speed profiles. The actual train power may be limited under the conditions of over voltage and over current.

The models of DC substation can be classified as non-reversible rectifiers or reversible DC/AC converter. Rectifiers are robust and reliable under low cost while the DC/AC converter is much expensive but they support bidirectional power flow and voltage regulation. In many cases, the open circuit voltage of the substation is assumed fixed at a given set point. Other voltage control methods can be used to improve the current and power sharing [15], [17]. However, dynamic voltage regulation is limited only to reversible substations.

This work studies the effects of the open circuit voltage of the DC substation on the system performance and efficiency under different testing conditions. The following parts of this paper are organized into three sections. The first section describes the mathematical models used for the substations, trains, and lines based on [9], [18]. The second section demonstrates the test cases and the results. The last section comments on the results and states the main conclusions.

Corresponding author: Bassam Mohamed

This work was partially supported by the Government of the Principality of Asturias - Foundation for Scientific and Technical Research (FICYT) under grants FC-GRUPIN-IDI/2018/000241 (Laboratory for Electrical Energy Management Unified Research (LEMUR)).

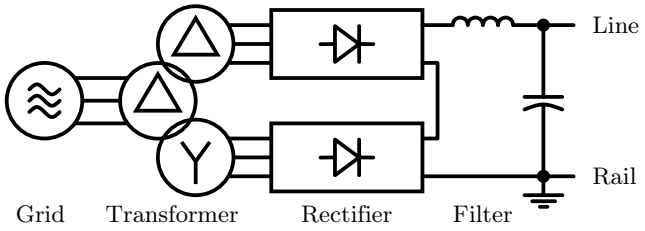

Fig. 1. Non reversible substation based on series rectifiers

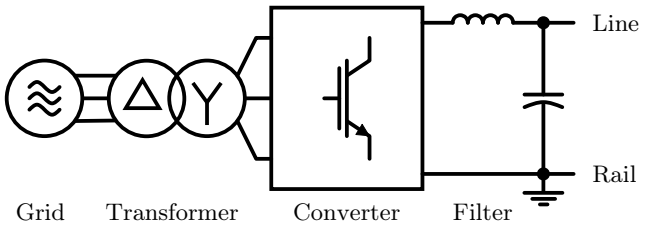

Fig. 2. Reversible substation based on AC/DC converter

II. Mathematical Models

A. Substation Model

The DC substations are designed to support three main functionalities. First, the DC substation should transfer the power from the AC grid (the main grid) to the DC network. The forward power flowing from the AC grid to DC network is used to feed the main demand of the DC traction network including the trains and losses. The second functionality of the DC substation is to provide the set point of the open circuit voltage level of the DC network which normally starts from 600 V up to 3000 V. The voltage regulation is required in many cases to avoid faults due to over current at excessive demand or over voltage caused by regenerative braking. In addition to those functionalities, some of the DC substations should be able to support the power transfer from the DC network to the AC grid. This reverse flow of power is required in some cases when the total regeneration braking power is higher than the total demand for trains and the losses.

Non-reversible DC substations are based on conventional three phase uncontrolled diode rectifiers. The majority of DC substations are designed based on this type because they are robust and reliable under low cost. However, they are limited to unidirectional power flow from the AC grid to the DC network. Another important problem is the harmonic injection at the AC grid caused by the nonlinear current consumption of the rectifier. Different configuration of multi-pulse rectifiers with LC filter can reduce the harmonic injection of low order. Fig. 1 shows an example of those configurations based on two series rectifiers. For this type of substations, the DC voltage depends on the AC voltage and winding ratio of the transformer. The tap changer of the transformer can be used to select the DC output voltage from preset values. This variation is slow and limited to because it is based on mechanical switching between different taps of the winding.

Reversible DC substations are designed to allow bidirectional power flow between the DC network and the AC grid. They are built using AC/DC converter based on controlled switching devices as shown at Fig. 2. In forward mode, the converter works as a rectifier with additional functionalities such as current shaping and harmonics elimination. In reverse mode, the converter injects active power back to the AC grid. In addition to normal operation, this converter can be used to regulate the DC voltage of the substation.

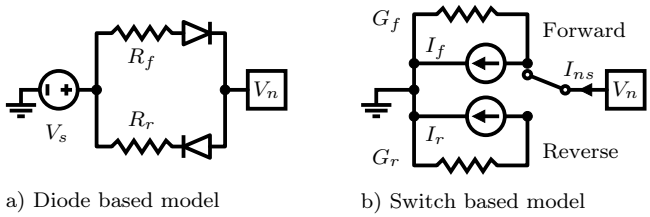

a) Diode based model b) Switch based model

Fig. 3. Simplification of the steady state model for the DC substation

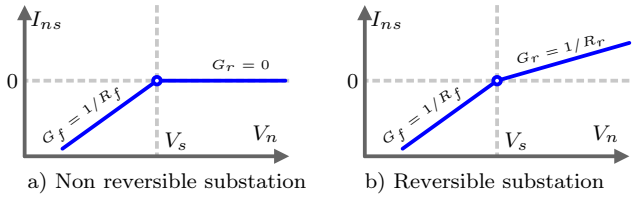

a) Non reversible substation b) Reversible substation

Fig. 4. The characteristic curve of $I_{ns}(V_n)$ for the DC substation

Fig 3 shows a simplified steady state model for the DC substation. The AC grid and transformers are represented by an equivalent DC slack voltage (V_s). This model assumes asymmetrical resistances for the bidirectional power flow. The forward mode parameters are marked by "f" subscript while the "r" subscript is used for the parameters of the reverse mode.

The equivalent Norton circuit is used to simplify the current injection formulation for each direction of the power flow. The ideal diodes are replaced by a simple voltage control switch. Eq(1) defines the shunt conductance (G_s) based on the mode of operation. Eq(4) uses the supper position principle to define the nodal injection current of the substation (I_{ns}) with two components.

The first component is the injection current from the slack (I_s) when the nodal voltage (V_n) is zero. The second component is the injection current from the DC network (I_n) when the slack voltage (V_s) is zero. Fig. 4.a shows a generalized model for the reversible substations. The conventional symmetrical power flow can be defined by assuming $(G_f = G_r)$ which is the most common case. In the case of the non-reversible substation, the (G_r) is assumed zero as shown in Fig. 4.b to prevent any reverse power flow.

$$G_s = \begin{cases} G_f & V_n < V_s \quad \text{Forward} \\ G_r & V_n \geqslant V_s \quad \text{Reverse} \end{cases} \tag{1}$$

$$I_s = G_s \times V_s \tag{2}$$

$$I_n = G_s \times V_n \tag{3}$$

$$I_{ns} = I_n - I_s \tag{4}$$

B. Train Model

The train model of this work is based on decoupling between mechanical and electrical models. The reference power of the train (P_{ref}) is estimated using a mechanical simulator. Fig.5.a shows the over current protection applied in demand mode

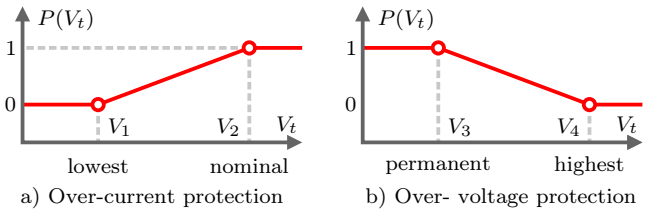

Fig. 5. The train protection curves for over-current and over-voltage

where $(P_{ref} > 0)$. The demanded power of the train is limited linearly if the train's voltage (V_t) is less than the normal level. The protection of the over voltage shown in Fig.5.b is activated in regeneration braking mode where $(P_{ref} < 0)$. The power injection of the train is reduced linearly if the train's voltage is higher than the permanent level. Eq(5) defines the train current (I_t) for a given reference power and operating voltage. Eq(6) defines the total injection current of all trains $(I_{nt}(m))$ connected to node (m).

$$I_t = (P(V_t) \bullet P_{ref}) \ / \ V_t \qquad \text{Train current} \qquad (5)$$

$$I_{nt}(m) = \underbrace{\sum I_t(k)}_{\mathbf{Node}(k) \equiv m} \qquad \text{Train injection current} \qquad (6)$$

C. Network Model

At each instant, the network topology should be updated based on the variation of trains positions. The line splitting algorithm divides the lines into segments and adds new intermediate nodes as required. Each line segment is represented by branch of a constant conductance (G_b) connected between source node **src** and destination node **dst**. Eq(7) defines the branch current based on Ohm's law. Eq(8) defines the total injection current of the branches connected to node (m). The branch current is assumed positive if it is going out of the node.

$$I_b = G_b \bullet (V_{\mathbf{src}} - V_{\mathbf{dst}}) \qquad \text{Branch current} \qquad (7)$$

$$I_{nb}(m) = \underbrace{\sum I_b(k)}_{\mathbf{src}(k)=m} - \underbrace{\sum I_b(k)}_{\mathbf{dst}(k)=m} \qquad \text{Branch injection current} \qquad (8)$$

D. MNA Solver with Adaptive Damping

The solver is based on MNA (Modified Nodal Analysis) with an adaptive damping method to overcome the divergence and oscillations caused by the non-smooth and non-linearity of the problem. Initially, the solver assumes a flat voltage profile for all nodes. At the start of each iteration, the solver updates the injection current of each element based on the models explained before. Then, the damping method is used to calculate the next step of the voltage vector based on the damping factor (α) as defined in Eq(9).

The solver updates this factor relative to the improvement in the convergence rate. The solver stops the iteration when the total error is less than the required tolerance. The full details of the mathematical models and the solver are explained at [9], [18], [19].

$$V_n = V_n^{old} + \alpha \cdot (V_n^{new} - V_n^{old}) \qquad (9)$$

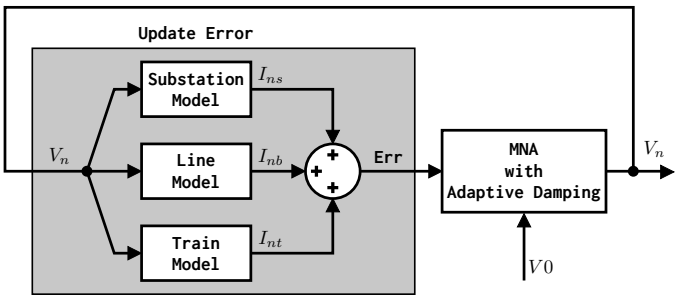

Fig. 6. The simplified diagram of the solver based on MNA

Require: V_s, R_s, P_{ref} , **Output:** V_n
1. **Initialize variables** $V_n = V0$
2. **Update substation injection current Eq.4**
3. **Update train injection current Eq.6**
4. **Update network injection current Eq.8**
5. **Update error** $Err = I_{ns} + I_{nt} + I_{nb}$
6. **Update** V_n **by MNA with Adaptive Damping**
7. **IF** $\parallel Err \parallel > \epsilon$ **GOTO** 2
8. **END**

Algorithm 1: Simplified power flow solver based on MNA with adaptive damping

III. Test Cases and Results

The test case (Fig. 7), represents a real 3000V DC traction network in the south of Spain. There are two tracks marked by blue and red dashed lines. The trips start from both ends every 20 minutes with 10 minutes shift for the red track. Each train has a peak of 2.2 MW for acceleration and 1.2 MW for regenerative braking. Each simulation covers a scheduled time of 200 minutes with a time step of one second. The solver tacks around 90 seconds to solve all instants for a single simulation. All branches have the same resistance per kilometers (R_b). There are 8 connection points but only 2, 4, and 7 are connected to DC substations. In forward mode, all DC substation acts as rectifiers with the same forward resistance (R_f). In reverse mode, only the fourth substation allows a limited power flow from the DC network to the AC grid with reverse resistance (R_r). In this case, there are no energy storage systems in the network, and all regenerative power must be consumed in the DC traction network or transferred to the AC grid. During the voltage sages $(0.66 \leqslant V_s \leqslant 0.76)$, the overcurrent protection prevents the trains from consuming the required power. The non-supplied power indicates that the timing of the schedule can not be achieved. Under the overvoltage conditions $(1.1 \leqslant V_s \leqslant 1.2)$, part of regenerative power must be burned by a resistor inside the train.

The test increments the slack voltage (V_s) from 0.9 pu to 1.1 pu with a step of 0.01 pu. Then, the test runs a full simulation for each value while keeping the other parameters as constant. The aggregated results of each simulation are saved and represented on the graph. Fig. 9 shows the variation of the results relative to the slack voltage in pu. The results represent the non-supplied

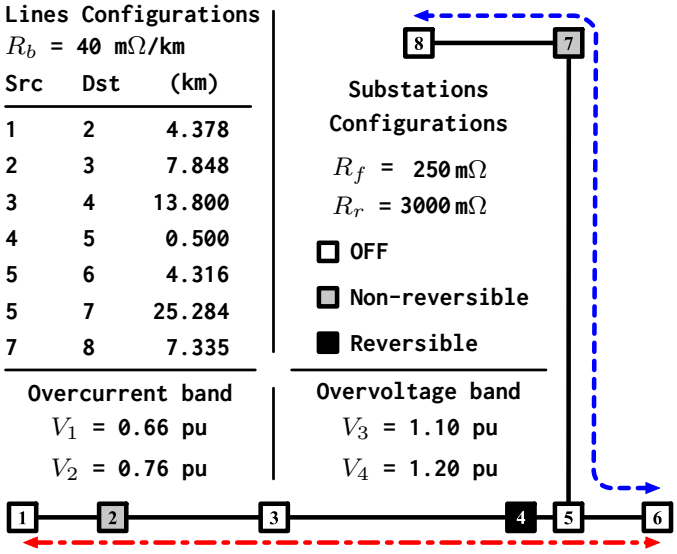

Fig. 7. The diagram and the configuration parameters of the test case

energy (E_N) in addition to the overall efficiency (η) and the total energy of the losses and consumption. Although, the non-supplied energy is not included in the total losses but it should be minimized to avoid the delays in the schedule due to the overcurrent protection. Even though the slack voltage is higher than 0.9 pu but the overcurrent protection is activated because of the network losses make the train voltage is much lower than that. Fig. 8 represents a simplified energy flow between the main elements in the Dc traction network. The AC grid provides the total energy consumption (E_{SI}) of the system while the reversible substations may inject back to the AC grid an extra recovered energy (E_{SO}) from regenerative braking. At the motor side of the train, (E_{TO}) represents the actual energy demand while (E_{TI}) represents the energy of regenerative braking. The line losses (E_{LL}) are proportional to the current because line impedance is purely resistive. In this case, the train model is represented as a constant power where the current will be reduced for the increment of the voltage. The same concept can be applied to the losses of the substations with some non-linearity because of the constant power model of the trains. Even though the higher voltage may reduce the losses of the substations and lines but it still not recommended because it may reduce the lifetime of the electric devices and the insulation materials. The train losses (E_{TL}) include the losses of the DC/AC converter and the burned energy due to over voltage at regenerative braking. The burned losses increase with the voltage because of the activation of the protection curve of the overvoltage. In this case, it is not applicable to avoid the burned losses because of the capacity limitation of the reversible substation. This problem can be solved by optimizing the schedule to synchronize the accelerating trains

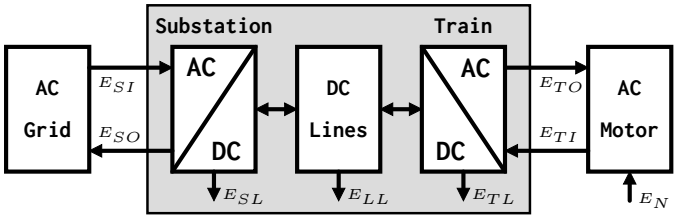

Fig. 8. Energy flow in a simplified DC traction network

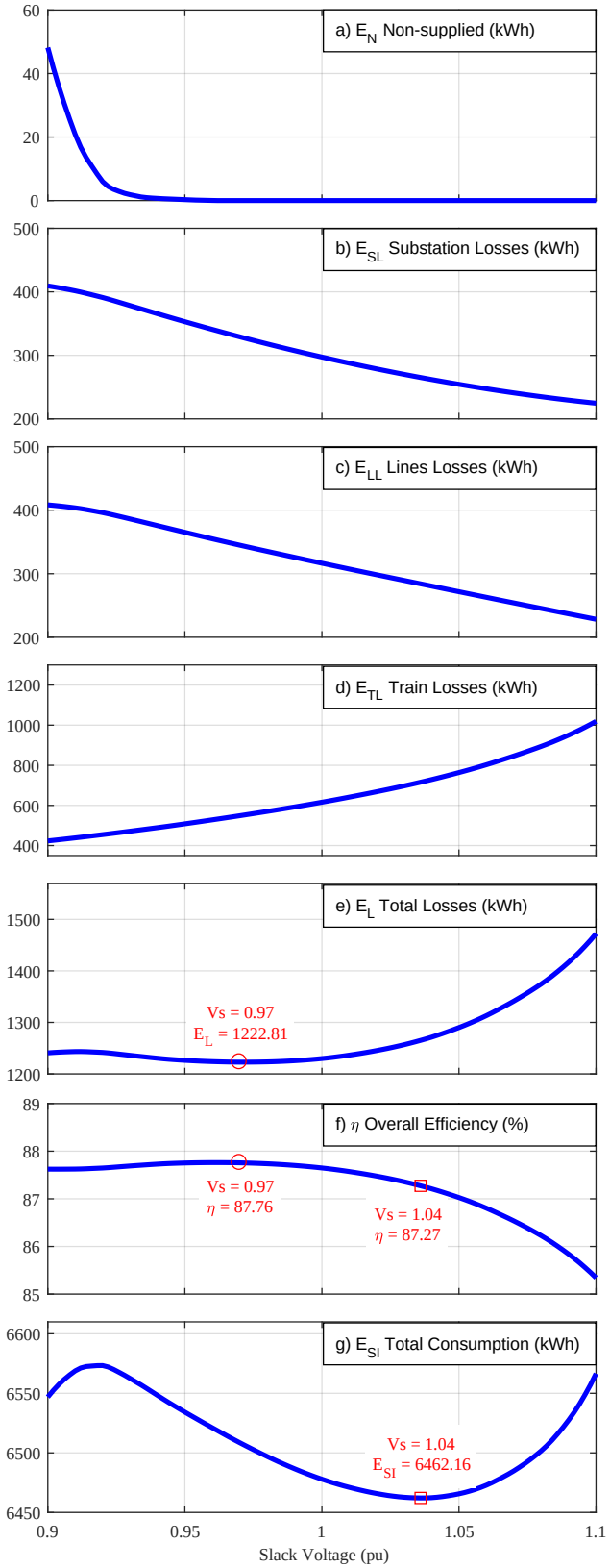

Fig. 9. The losses variation relative to the slack voltage

with other adjacent trains under regenerative braking. However, this solution requires trains with auto driving which still not available for all cases.

The total losses represent the losses summation of DC lines (E_{LL}), substation (E_{SL}), and trains (E_{TL}). The curve of the total losses starts as a horizontal line. Then, it increases exponentially because of the excessive activation of the overvoltage protection.

Eq(10) defines the overall energy efficiency (η) based on the total input and output energies to the DC system. In this case, the maximum efficiency achieved at ($Vs = 0.97pu$) which represents the minimum point of the total losses. The selection of the slack voltage should avoid the activation of overcurrent protection to achieve the required schedule timing. As shown in Fig. 9.a, this condition is fulfilled for all slack voltages higher than 0.95 pu because the non-supplied energy (E_N) tends to zero beyond this limit. The minimization of the total energy consumption (E_{SI}) is an important aspect of the operation because in many cases the cost of energy depends only on the measurements of the energy injected into the DC network.

In this case, the minimum energy consumption (E_{SI}) is achieved at ($V_s = 1.04$) with a reduction of efficiency by 0.5 %. The higher voltage profile may cause overheating in the trains due to the burned energy of extra regenerative braking. It is a trad of requirements and regulations to select operation point at the maximum efficiency or the minimum cost.

$$\eta = \quad 100 \times \frac{E_{SO} + E_{TO}}{E_{SI} + E_{TI}} \qquad \text{Total Energy Efficiency} \tag{10}$$

IV. Conclusion

This work studies the effects of the selection of the open circuit voltage of the DC substation. During this study, the simulator has to solve hundreds of thousands of instants which requires huge data size for the results and extended simulation time. The study improves the simulation speed by using simplified models with accepted accuracy for steady state analysis. Based on this simplification, the simulator was able to solve more than hundred instants per second. The aggregated data are used to minimize the size required for saving the results. Few aggregated values can be used to represent the total losses of full simulation.

Finally, each simulation is represented by a single point on the plot. The testing steps are designed to be generic so that it can be applied in any case without restrictions or specific formulation. Based on the results of this study, there is a set point of the open circuit voltage of the DC substations which can achieve the maximum overall efficiency fixed network configurations and timing schedules.

Acknowledgment

The authors would like to thank CAF Turnkey & Engineering, specially to Peru Bidaguren for his support during the development of these models.

References

[1] Z. Tian, G. Zhang, N. Zhao, S. Hillmansen, P. Tricoli, and C. Roberts, ''Energy evaluation for DC railway systems with inverting substations,'' in *2018 IEEE International Conference on Electrical Systems for Aircraft, Railway, Ship Propulsion and Road Vehicles International Transportation Electrification Conference (ESARS-ITEC)*, Nov. 2018.

[2] M. Khodaparastan, A. A. Mohamed, and W. Brandauer, ''Recuperation of regenerative braking energy in electric rail transit systems,'' *IEEE Transactions on Intelligent Transportation Systems*, vol. 20, no. 8, pp. 2831--2847, 2019.

[3] C. J. Goodman and L. K. Sin, ''DC railway power network solutions by diakoptics,'' in *Proceedings of IEEE/ASME Joint Railroad Conference*, Mar. 1994, pp. 103--110.

[4] M. T. Söylemez, S. Aç, and Others, ''Multi-train simulation of DC rail traction power systems with regenerative braking,'' *WIT Transactions on The Built Environment*, vol. 74, 2004.

[5] V. Acary, O. Bonnefon, and B. Brogliato, *Nonsmooth Modeling and Simulation for Switched Circuits*, ser. Lecture Notes in Electrical Engineering. Springer Netherlands, 2012.

[6] E. Ngoya, J. Rousset, and J. J. Obregon, ''Newton-raphson iteration speed-up algorithm for the solution of nonlinear circuit equations in general-purpose cad programs,'' *IEEE Transactions on Computer-Aided Design of Integrated Circuits and Systems*, vol. 16, no. 6, pp. 638--644, 1997.

[7] Z. Liu, X. Zhang, M. Su, Y. Sun, H. Han, and P. Wang, ''Convergence analysis of newton-raphson method in feasible power-flow for dc network,'' *IEEE Transactions on Power Systems*, pp. 1--1, 2020.

[8] Chung-Wen Ho, A. Ruehli, and P. Brennan, ''The modified nodal approach to network analysis,'' *IEEE Transactions on Circuits and Systems*, vol. 22, no. 6, pp. 504--509, 1975.

[9] B. Mohamed, P. Arboleya, and C. González-Morán, ''Modified current injection method for power flow analysis in heavy-meshed dc railway networks with nonreversible substations,'' *IEEE Transactions on Vehicular Technology*, vol. 66, no. 9, pp. 7688--7696, 2017.

[10] Y. Cai, M. R. Irving, and S. H. Case, ''Modelling and numerical solution of multibranched dc rail traction power systems,'' *IEE Proceedings - Electric Power Applications*, vol. 142, no. 5, pp. 323--328, 1995.

[11] C. L. Pires, S. I. Nabeta, and J. R. Cardoso, ''ICCG method applied to solve DC traction load flow including earthing models,'' *IET Electr. Power Appl.*, vol. 1, no. 2, pp. 193--198, Mar. 2007.

[12] W. Liu, Q. Li, and M. Chen, ''Study of the simulation of dc traction power supply system based on ac/dc unified newton-raphson method,'' in *2009 International Conference on Sustainable Power Generation and Supply*, 2009, pp. 1--4.

[13] C. L. Pires, S. I. Nabeta, and J. R. Cardoso, ''Dc traction load flow including ac distribution network,'' *IET Electric Power Applications*, vol. 3, no. 4, pp. 289--297, 2009.

[14] P. Arboleya, G. Diaz, and M. Coto, ''Unified ac/dc power flow for traction systems: A new concept,'' *IEEE Transactions on Vehicular Technology*, vol. 61, no. 6, pp. 2421--2430, 2012.

[15] F. Hao, G. Zhang, J. Chen, Z. Liu, D. Xu, and Y. Wang, ''Optimal voltage regulation and power sharing in traction power systems with reversible converters,'' *IEEE Transactions on Power Systems*, pp. 1--1, 2020.

[16] C. Mayet, P. Delarue, A. Bouscayrol, E. Chattot, and J. Verhille, ''Comparison of different emr-based models of traction power substations for energetic studies of subway lines,'' *IEEE Transactions on Vehicular Technology*, vol. 65, no. 3, pp. 1021--1029, 2016.

[17] S. Aatif, H. Hu, X. Yang, Y. Ge, Z. He, and S. Gao, ''Adaptive droop control for better current-sharing in VSC-based MVDC railway electrification system,'' *Journal of Modern Power Systems and Clean Energy*, vol. 7, no. 4, pp. 962--974, Jul. 2019.

[18] P. Arboleya, B. Mohamed, and I. El-Sayed, ''DC railway simulation including controllable power electronic and energy storage devices,'' *IEEE Trans. Power Syst.*, vol. 33, no. 5, pp. 5319--5329, Sep. 2018.

[19] B. Mohamed, I. El-Sayed, and P. Arboleya, ''DC railway infrastructure simulation including energy storage and controllable substations,'' in *2018 IEEE Vehicle Power and Propulsion Conference (VPPC)*, Aug. 2018, pp. 1--6.